Developmental Biology **207,** 457–469 (1999)
Article ID dbio.1998.9172, available online at http://www.idealibrary.com on IDEAL®

Functional Roles of Calcium Channel α_1 Subunits in Sperm

Ruth E. Westenbroek* and Donner F. Babcock†,[1]

**Department of Pharmacology and †Physiology and Biophysics, University of Washington, Seattle, Washington 98195*

The Ca channels of male germ-line cells are partially characterized, but the molecular properties and subcellular localization of the Ca channels of mature sperm are unknown. Here, we probe rodent sperm with anti-peptide antibodies directed to cytosolic domains of cloned rat brain α_{1A}, α_{1C}, and α_{1E} Ca channel subunits. Each recognizes a 200- to 245-kDa band on immunoblots of whole rat sperm extracts. A smaller (~110-kDa) α_{1C} band also is detected. Confocal fluorescence images of mouse sperm show characteristic patterns of punctate α_{1A}-, α_{1C}-, and α_{1E}-immunoreactivity. For α_{1A}, the puncta are larger, less numerous, and more variable in distribution than for α_{1C} and α_{1E}. They are absent from the acrosomal crescent, but are present elsewhere over the sperm head, often at the apical tip and equatorial segment. They also are found at irregular intervals along both the midpiece and the principal piece of the flagellum. For α_{1C} and α_{1E}, puncta are dense along dorsal and ventral aspects of the acrosomal cap. For α_{1E} but not α_{1C}, the remainder of the acrosomal region also is labeled. Neither is found in the postacrosomal region or on the midpiece. Puncta of α_{1C} and α_{1E} occur at regular intervals each in two parallel rows, at the dorsal and ventral aspects of the proximal segment of the flagellar principal piece. The puncta in these arrays become less abundant and intense in the distal flagellum. These results demonstrate that multiple Ca channel proteins are present in mature sperm and are regionally localized in ways that may give them different regulatory roles.

INTRODUCTION

Current understanding of the molecular basis of fertilization indicates that diverse receptors are activated and multiple downstream signaling pathways are engaged in sperm preparing for their final encounter with the egg (Ward and Kopf, 1993; Snell and White, 1996). Sperm possess counterparts to many of those components of somatic cells that control protein phosphorylation status and the production and degradation of cyclic nucleotide and lipid-derived messengers. Several of these signaling effectors exist as unique isoforms in sperm (da Cruz e Silva *et al.*, 1995; Berruti and Borgonovo, 1996; Naro *et al.*, 1996) or are regionally distributed (Lieberman *et al.*, 1988; Walensky *et al.*, 1996; Mei *et al.*, 1997; Sallese *et al.*, 1997; Vijayaraghavan *et al.*, 1997; Zini *et al.*, 1997) in ways that suggest particular roles in the control of metabolism, motility, or acrosomal exocytosis in these highly polarized cells. Less is known of the channels, pumps, and exchangers that determine ionic responses in sperm. Because Ca^{2+} entry mediates fertilization and both the changes in sperm swimming behavior and the acrosomal exocytosis that precede it, ignorance of the properties, distributions, and regulation of sperm Ca channels is a particularly prominent impediment.

Voltage-gated Ca currents of somatic cells are assigned to class L, N, P/Q, R, or T based on pharmacological sensitivities and other properties observed by patch clamp methods (De Waard *et al.*, 1996). Patch clamp studies of cells transfected with the coding regions of the eight known genes that specify the pore-forming Ca channel α_1 subunit ($\alpha_{1A, B, C, D, E, G, H, or S}$) indicate correlation of expression of α_{1C}, α_{1D}, and α_{1S} with L-type, α_{1B} with N-type, α_{1A} with P/Q-type, and the newfound α_{1G} and α_{1H} (Perez-Reyes *et al.*, 1998; Cribbs *et al.*, 1998) with T-type currents. Correspondence of α_{1E} expression with R- or perhaps T-type currents remains

[1] To whom correspondence should be addressed at Department of Physiology and Biophysics 357290, University of Washington, Seattle, WA 98195-7290. Fax: (206)-685-0619. E-mail: donner@u.washington.edu.

0012-1606/99 $30.00

controversial (Bourinet *et al.*, 1996; Randall and Tsien, 1997; Perez-Reyes *et al.*, 1998; Meir and Dolphin, 1998).

Characterization of the Ca channels of sperm presents special problems. The highly differentiated and motile nature of these cells has prevented patch clamp recordings except in exceptional circumstances (Babcock *et al.*, 1992). The transcriptional and translational inactivity of sperm also prohibits examination by both cloning and transfection strategies. Early examination of the pharmacological sensitivity of Ca^{2+} entry by optical methods indicated that L-type Ca channels of sperm have required roles in acrosomal exocytosis (Babcock and Pfeiffer, 1987; Florman *et al.*, 1989, 1992). However, more recent efforts have focused on the germ-line cells from which sperm arise. Study of patch-clamped spermatocytes and round spermatids revealed only T-type Ca currents (Hagiwara and Kawa, 1984; Santi *et al.*, 1996; Arnoult *et al.*, 1996, 1997) and only transcripts of α_{1E} and α_{1A} subunits were detected in spermatogenic cell extracts (Liévano *et al.*, 1996). Although evidence of an expressed α_{1E} protein in mature sperm was not provided, it was proposed that α_{1E} subunits are retained during spermiogenesis and that mature sperm possess only T-type channels. Thus, the identity of sperm Ca channels remains clouded.

Here we apply a panel of antibodies specific for various α_1 subunits to ask directly which Ca channel proteins are present in rodent epididymal sperm, to estimate their molecular mass, and to determine their distributions on the cell surface. We find that sperm possess α_{1A}, α_{1C}, and α_{1E} subunit proteins of apparent sizes similar to those reported for somatic cells. We also find that localization patterns for α_1 subunits follow established regional boundaries (Bartles, 1996; Cowan *et al.*, 1997) to the mobility of sperm surface proteins. These results demonstrate that multiple Ca channel polypeptides are present in mature sperm and are distributed among sites that may allow localized entry of Ca^{2+} to selectively control metabolic, kinetic, and secretory activity of these cells.

MATERIALS AND METHODS

Materials

Vectashield, biotinylated anti-rabbit IgG, and avidin D–fluorescein were from Vector. Purified AKAP82 and anti-AKAP82 antibody were generous gifts of Dr. S.B. Moss. Calpain I and II were from Calbiochem, leupeptin and aprotinin were from Boehringer Mannheim, and ECL reagent was from Amersham. All other chemicals were from Sigma.

Sperm Preparation and Incubation Conditions

Cauda epididymides and proximal vas deferens were excised from male Swiss Webster (retired breeder) mice or from ~300-g male Sprague–Dawley rats and transferred to Medium HS that contained (in mM): 125 NaCl, 5 KCl, 2 $CaCl_2$, 1 $MgCl_2$, 30 Hepes, 10 lactic acid, 1 pyruvic acid, pH 7.4. After removal of adherent connective, circulatory, and adipose tissue, the cleaned organ pairs were transferred to a collection medium.

Mouse epididymal semen was allowed to exude (15 min at 37°C in a 5% CO_2/95% air atmosphere) from three to five small incisions into 1 ml of a collection medium consisting of Medium HS supplemented with 15 mM $NaHCO_3$ and 5 mg BSA (Fraction V)/ml. All subsequent operations were conducted at room temperature and used Medium HS. The suspension was twice diluted to 3 ml and cells were collected by sedimentation (600*g*, 5 min). The washed sperm were dispersed and stored in 0.6 ml (1–2 $\times$ 10^6 cells/ml).

Each cleaned rat epididymis was transferred to a 35-mm plastic culture dish containing ~1 ml of a collection medium that contained (in mM): 135 NaCl, 5 KCl, 2 EGTA, 1 $MgCl_2$, 10 Hepes, pH 7.4. Rat semen was extruded from a single small incision at the flexure of the caudal epididymis by retrograde perfusion through the vas deferens. The ropy exudate was dispersed by gentle swirling and diluted to ~9 ml with cooled (4°C) collection medium that was fortified with protease inhibitors (in μg/ml): 10 leupeptin, 690 pepstatin, 10 calpain inhibitors I and II, 100 benzamidine, 20 aprotinin, 34 PMSF, 198 phenanthroline. Cells were washed twice by dilution and sedimentation (600*g*, 5 min) and then resuspended directly into SDS sample buffer: 80 mM Tris–HCl, 1 mM EDTA, 10 mM DTT, 2% SDS, 10% glycerol, pH 6.7.

Immunolocalization

Aliquots (120 μl) of washed, diluted (0.2–0.5 $\times$ 10^6 cells/ml) mouse epididymal sperm were dispensed onto cooled (4°C) 12-mm round coverslips and allowed to settle for 5–15 min. To reveal the cytosolic epitopes of interest, settled sperm were fixed in 4% paraformaldehyde for 1 h, rinsed in PBS[2] (5$\times$ 3 min), permeabilized with 0.05% Triton X-100 in PBS for 15 min, washed in PBS (5$\times$ 3 min), blocked for 1 h in PBS containing 5% nonfat milk and 1% BSA, and rinsed in PBS for 15 min. These fixed, permeabilized samples were then incubated with the affinity-purified antibodies CNC1, CNE2, or CNA5, whose preparation and characterization were described previously (Hell *et al.*, 1993; Yokoyama *et al.*, 1995; Sakurai *et al.*, 1996). All antibodies were diluted 1:15 (30–133 μg/ml) in PBS containing 1% BSA. After 1 h at 22°C and overnight at 4°C, samples were rinsed in PBS (6$\times$ 5 min) and incubated in biotinylated anti-rabbit IgG (diluted 1:300) for 1 h at 37°C. The samples were rinsed in PBS (6 $\times$ 5 min), incubated in avidin D fluorescein (diluted 1:300) for 1 h at 37°C, rinsed with PBS (2$\times$ 5 min), PB (3$\times$ 5 min), and finally rinsed with distilled water. These processed coverslips were inverted onto a glass slide and affixed with Vectashield mounting medium. Images were collected with 1.4 NA, 60X or 100X objectives (Nikon) on a Bio-Rad MRC 600 confocal microscope, adjusted to provide optical sections of 0.7 μm, at the Keck Imaging Facility of the University of Washington.

Controls for nonspecific staining included specimens processed as described above except for deletion of the primary antibody or by its replacement with peptide-blocked primary antibody, prepared by incubation for 6–8 h with a 20 μM concentration of the corresponding peptide or fusion protein. In all cases, observed residual staining was negligible. Controls using preimmune serum also showed neglible staining.

[2] Abbreviations used: PB, 10 mM sodium phosphate buffer, pH 7.4; PBS, phosphate-buffered saline; TBS, Tris-buffered saline; TBST, TBS with 0.05% Tween 20; SDS, sodium dodecyl sulfate.

Image Analysis

The periodic spacing of immunoreactive puncta in 3- to 5-μm proximal segments of the flagellar principal piece was identified objectively from prominent peaks in the power spectra generated by fast Fourier transforms (Origin, Microcal) of normalized emission intensity from parallel line scans (Metamorph, Universal Imaging) in dorsal and ventral regions of equal area (64–128 × 4–6 pixels) along the flagellar axis. Dorsal and ventral periodicities from each cell (n = 11–16) were averaged and converted to absolute distances using calibration parameters determined from reflected light images of a ruled glass scale (Noran) examined at various hardware zoom settings (2.0–3.4). Axial displacement of puncta in these arrays was examined by cross-correlation analysis (Igor, Wavemetrics) after geometrical alignment of the origin of dorsal and ventral line scans to the junction of the flagellar midpiece and principal piece (the annulus).

Immnunoblot analysis

Suspensions of rat sperm (~1 μg protein) in SDS sample buffer were sonicated briefly, heated for 30 min at 50–60°C, and then applied to 5% polyacrylamide gels, along with M_r marker proteins and authentic affinity-purified rat brain Ca channel proteins (Westenbroek *et al.*, 1992). After electrophoretic separation, proteins were transferred onto nitrocellulose in buffer containing: 12.5 mM Tris, 96 mM glycine, 0.1% SDS, 15% (v/v) methanol, pH 8.3. After incubation in TBS containing 10% nonfat powdered milk (1 h, 22°C), the blocked membranes were transferred to fresh medium supplemented with 10–20 μg/ml of CNA5, CNC1, or CNE2 antibodies. Incubation continued for a further 80 min. After being rinsed in fresh antibody-free medium, membranes were incubated with HRP–protein A (diluted 1:1000) for 1 h, washed for 2.5 h in TBS containing 0.05% Tween 20, and then developed with ECL reagent. In other experiments using similar protocols, dot blots of mouse AKAP82 and the CNC1, CNE2, and CNA5 oligo- or polypeptides were probed with CNC1, CNA5, CNE2, or anti-AKAP82 antibodies. Specifically, serial dilutions (50 ng/μl–5 fg/μl) of each antigen were dried onto nitrocellulose, blocked (5% nonfat milk for 30 min), rinsed in TBST (TBS plus 0.05% Tween 20) for 30 min, and then incubated either with anti-AKAP82 (1:5000 dilution) or with 1:25 dilutions (10 μg/ml) of CNC1, CNE2, or CNA5 antibodies for 1 h. After being rinsed in TBST, membranes were incubated with HRP–protein A, washed in TBST for 30 min, and then developed with ECL reagent.

RESULTS

Much indirect evidence indicates that voltage-gated Ca channels of sperm have required functional roles in the events that occur between mating and fertilization. However, remarkably little is known of the molecular nature of these channels. Their distribution on the cell surface, a probable determinant of their regulatory roles, also is unknown. To characterize the properties and distribution of Ca channel proteins, we have probed rodent sperm with antibodies raised against peptides from signature regions of the predicted amino acid sequences of three cloned α_1-subunits of rat brain Ca channels.

Characteristic Patterns of Ca Channel α_1 Subunit Immunoreactivity in Sperm

Figure 1 shows representative confocal α_{1C}, α_{1E}, and α_{1A} immunofluorescence images of mouse epididymal sperm, observed in optical sections chosen to allow simultaneous examination of head and flagellum. Controls (right column) using antibodies blocked by prior exposure to the peptide antigen showed only low, uniform fluorescence, indicating a high level of specificity in the detected signal, consistent with previous validations of these probes (Hell *et al.*, 1993; Yokoyama *et al.*, 1995; Sakurai *et al.*, 1996). Controls using preimmune serum also produced neglible staining (data not shown). In all cases, specific immunoreactivity (left column) was punctate and regionally localized in both the sperm head and tail. For α_{1C} and α_{1E}, small (<0.3-μm-diameter) puncta were found in the acrosomal, but seldom in the postacrosomal, segment of the head. For α_{1C}, staining was confined mostly to the acrosomal crescent. In the flagellum, puncta of α_{1C} and α_{1E} were absent from the midpiece, but present at both the dorsal and ventral surface of the principal piece. Staining was more intense and regular in the proximal than in the distal segment. For α_{1A}, larger (~0.6-μm-diameter) puncta were present in both the acrosomal and postacrosomal head, but absent from the surface overlying the acrosome. The most intense staining often was found at the apical tip, along the equatorial segment, and at the connecting piece where the head joins the midpiece. Similarly large puncta were abundant in the midpiece and variably present in the principal piece of the flagellum. Figure 1 thus reveals that characteristic patterns of α_{1A}-, α_{1C}-, and α_{1E}-immunoreactivity follow sharp regional boundaries which separate the acrosome from the remainder of the anterior head, the acrosomal from the postacrosomal head, the head from the midpiece, and the midpiece from the principal piece of the flagellum.

During these experiments, we observed that staining patterns in the sperm head were quite dependent on the optical plane of the confocal section examined. Figures 2, 4, and 5 document these observations. Figure 3 examines Ca channel subunit localizations to the flagellum in more detail.

Localization of Ca Channel α_{1C} Subunits in Sperm

Figures 2A, 2B, and 2C show α_{1C} immunoimages obtained at focal planes of increasing distance from the proximal surface of the head of a representative sperm (z-series). Staining of the dorsal aspect of the acrosomal crescent was densest in central optical sections (Fig. 2B). Staining of the ventral aspect was densest in the proximal sections (Fig. 2C), decreasing as the plane of focus descended through the cell to the supporting surface. These patterns are most consistent with a localization of α_{1C} subunits to regions where outer acrosomal and plasma membranes are in close proximity. Figure 2D is a projection of this z-axis series. It offers a useful representation of the overall distribution of

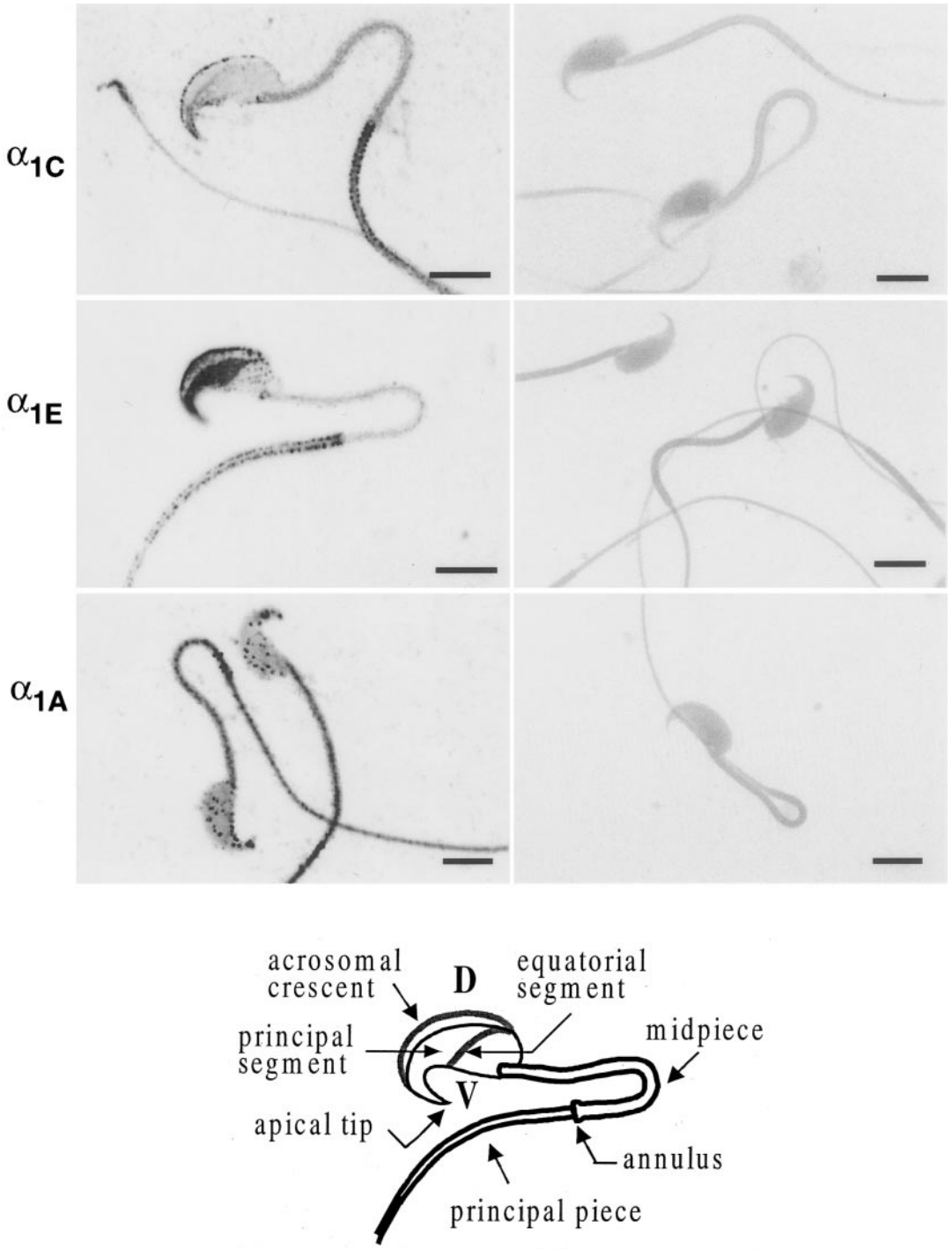

FIG. 1. Distinct patterns of immunolocalization of Ca channel α-1 subunits in mouse sperm. Representative confocal immunofluorescence images are shown in reverse contrast for cells treated with antibodies directed to α_{1C}, α_{1E}, or α_{1A}, applied alone (left) or after blocking with the peptide or fusion protein antigen (right). Scale bars are 5 μm. Anatomical nomeclature and relevant features of mouse sperm morphology are indicated in the line drawing at the bottom. The equatorial segment divides the sperm head into acrosomal and postacrosomal domains. The annulus divides the flagellum into midpiece and principal piece. Dorsal (D) and ventral (V) surfaces are indicated.

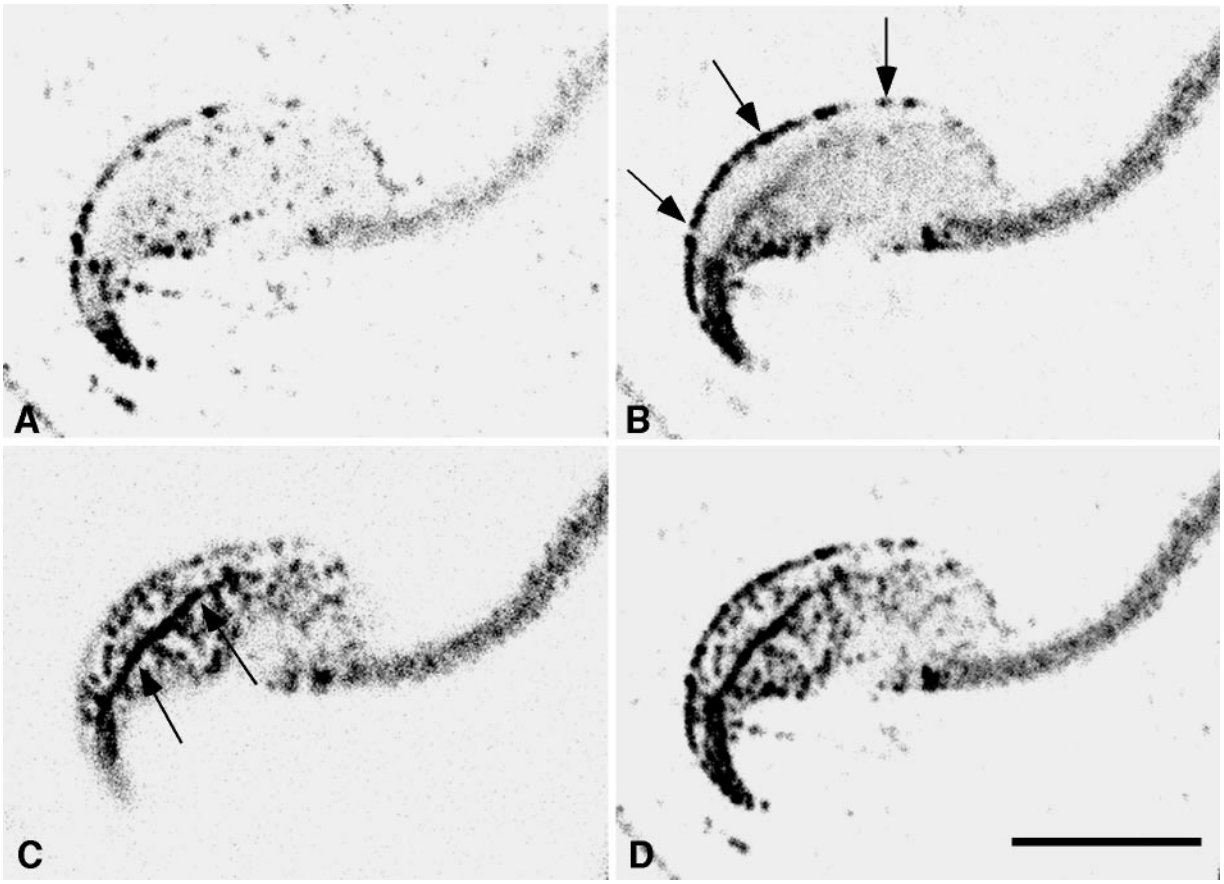

FIG. 2. Ca channel α_{1C} subunits overlie the acrosome. Confocal immunofluorescence images of a cell treated with antibodies directed to rat brain α_{1C}. Shown are distal (A), central (B), and proximal (C) *z*-axis optical sections (each separated by 1 μm), and a projection of the three (D). The arrows in B and C mark dorsal and ventral aspects of the acrosomal crescent, respectively. Scale bar is 5 μm.

α_{1C} immunoreactivity in the sperm head, but obscures some of the details apparent in single optical sections.

Figures 3A and 3B show immunoimages from two cells that are typical of those obtained when the focal plane is chosen to optimize visualization of α_{1C}-immunoreactivity in the sperm flagellum. The relatively low-magnification images (left panels) confirm the strong localization of α_{1C} puncta to the principal piece observed in Fig. 1. In expanded scale images (right panels), a periodic distribution of puncta along the dorsal and ventral aspects of the proximal segment of the principal piece is more evident. To determine the imperfectly regular spacing between puncta in these regions, we examined the power spectrum of Fourier transforms of emission intensity along the flagellar axis. The indicated mean periodicity was 0.57 ± 0.02 μm ($n = 15$). Cross-correlation analysis of these data did not reveal any bias in the alignment of dorsal and ventral puncta, indicating that each array originates at approximately the same distance from the junction of the midpiece to the principal piece. Thus, α_{1C} subunits are arranged in parallel arrays of puncta, whose size is near or below the limits of optical resolution.

Localization of Ca Channel α_{1E} Subunits in Sperm

Figure 4 shows a *z*-series of α_{1E} immunoimages and their projection. As for α_{1C}, the ventral aspect of the acrosomal crescent is most heavily stained in proximal optical sections (Fig. 4C). However, unlike α_{1C}- (Fig. 2), α_{1E}-immunoreactivity also was present in the remainder of the acrosomal region of the head. The dorsal aspect of the acrosomal crescent was most strongly stained at a central plane of focus, whereas staining of the rest of the anterior head (the principal segment) was diminished (Fig. 4B), consistent with localization to surface membranes. In the most distal sections (Fig. 4A), staining of the anterior head was again stronger. Comparison of the *z*-series projections of α_{1C} and α_{1E} immunoimages (Figs. 2D and 4D) clearly shows that α_{1E} is not restricted to membranes that overlie the acrosome, suggesting that it may have roles other than in acrosomal exocytosis.

Figures 3C and 3D show representative low- and high-magnification α_{1E} immunoimages of the flagella of two cells. Like α_{1C} (Figs. 3A and 3B), α_{1E} puncta were distributed

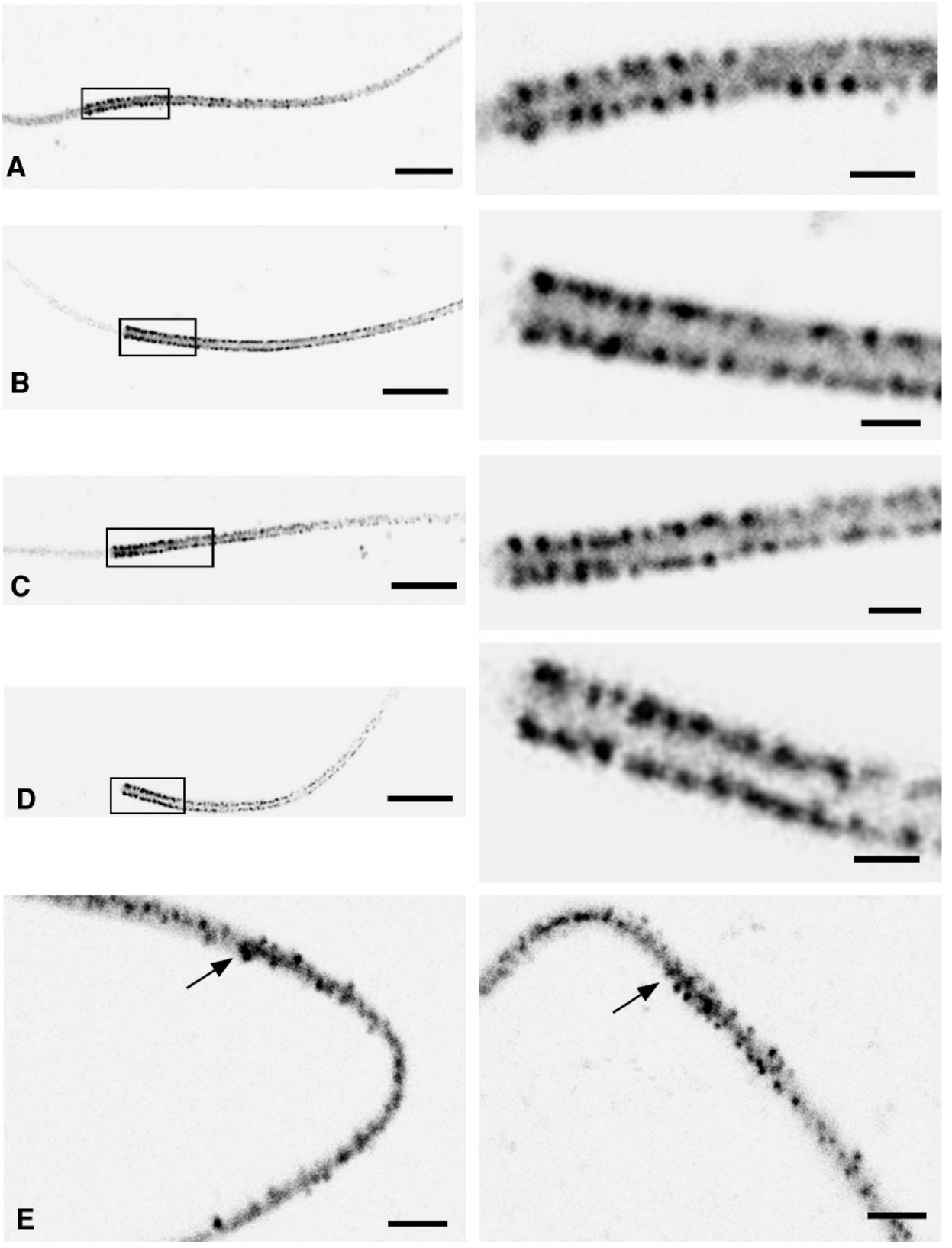

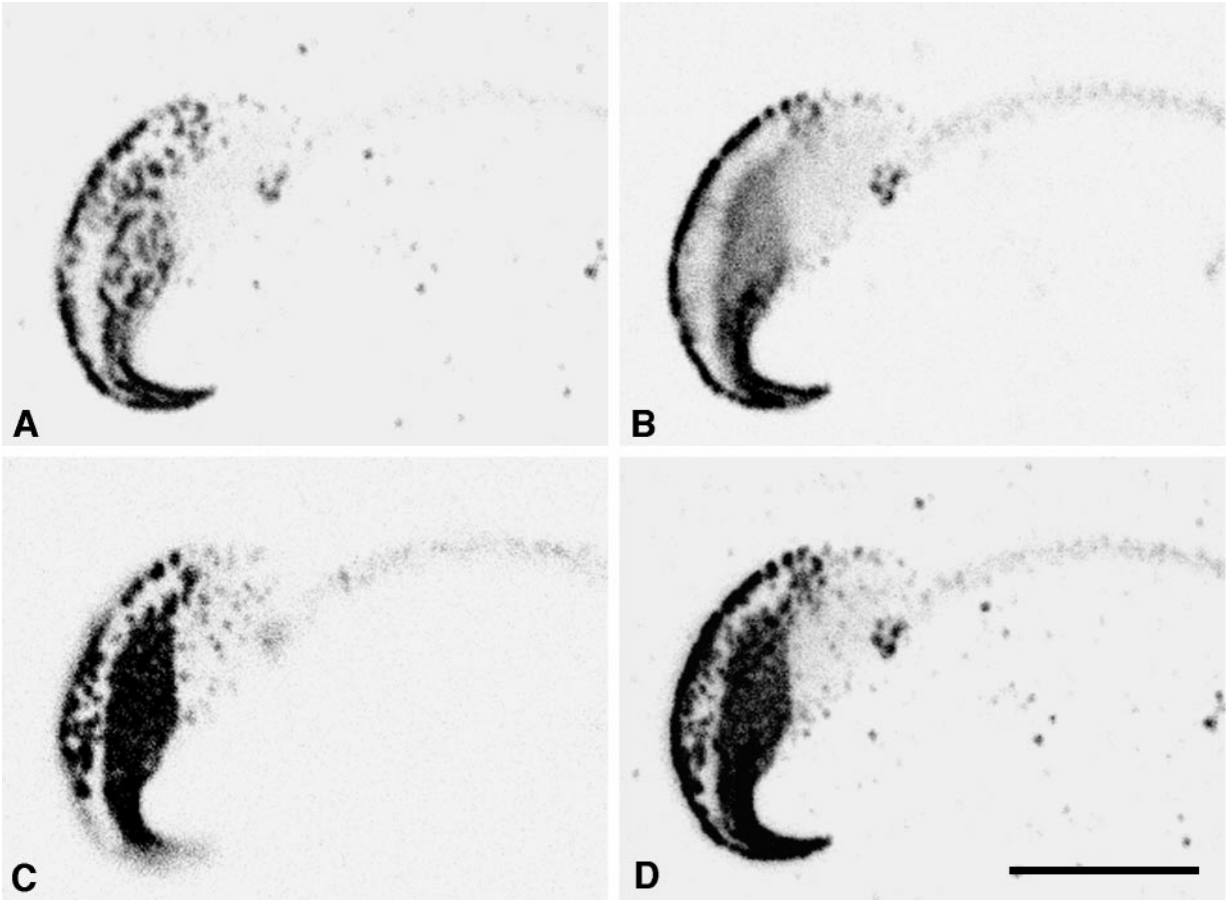

FIG. 4. Ca channel α_{1E} subunits in the acrosomal segment. Confocal immunofluorescence images of a cell treated with antibodies directed to rat brain α_{1E}. Shown are distal (A), central (B), and proximal (C) *z*-axis optical sections and a projection of the three (D) as in Fig. 2. Scale bar is 5 μm.

along the dorsal and ventral aspects of the proximal segment of the principal piece. Power spectrum and cross-correlation analyses indicated that α_{1E} subunits also are arranged in parallel arrays of puncta with a mean axial spacing of 0.54 ± 0.02 μm (n = 11), indistinguishable from that determined for α_{1C}.

These results suggest that Ca channels in the principal piece may be organized by association with cytoskeletal elements or structural components of the flagellum itself. The fibrous sheath, which underlies the plasma membrane of the principal piece, is a likely candidate for such an organizing role. It consists of two longitudinal columns, laterally cross-connected by ribs which are spaced at approximately the same interval (Fawcett, 1975; Toshimori *et al.*, 1985; Eddy and O'Brien, 1994) as that found for α_{1C} and α_{1E} puncta. Moreover, the major peptide component of the fibrous sheath is a member of the AKAP anchoring protein family (Carrera *et al.*, 1994; Johnson *et al.*, 1997b; Mei *et al.*, 1997).

Localization of Ca Channel α_{1A} Subunits in Sperm

Figure 5 shows a *z*-series of α_{1A} immunoimages and their projection. Distal, central, and proximal optical sections

FIG. 3. Punctate distribution of Ca channel α_1 subunits in the sperm flagellum. Confocal immunfluorescence images of two cells treated with antibodies directed to rat brain α_{1C} (A, B) or α_{1E} (C, D). The boxed regions that enclose the proximal principal piece (left) are shown at higher magnification (right). Scale bars are 5 and 1 μm, respectively. In the lower magnification images of two cells treated with antibodies to α_{1A} (E) arrows mark the annulus at the junction of the midpiece (right) and principal piece (left). Scale bars are 5 μm.

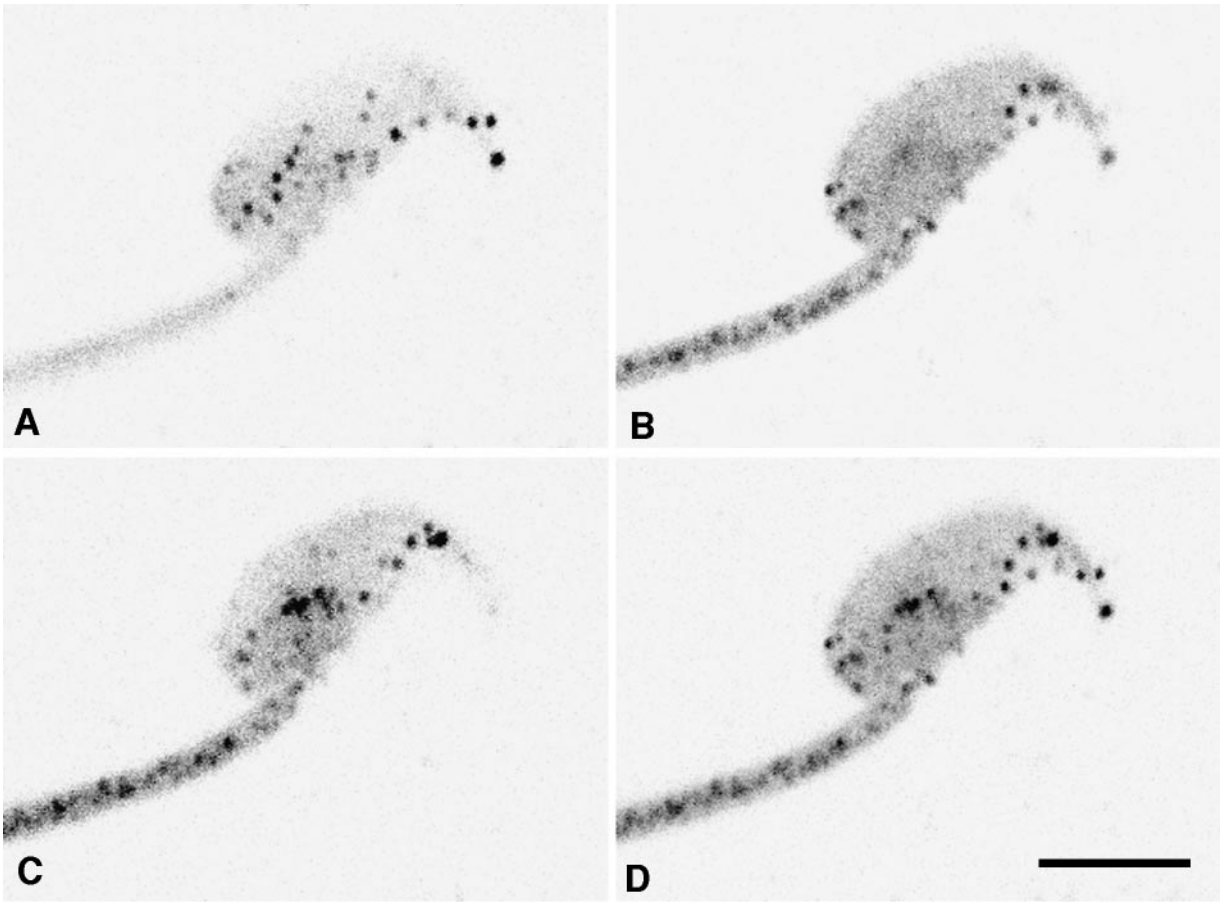

FIG. 5. Ca channel α_{1A} subunits in the apical tip and equatorial segment. Confocal immunofluorescence images of a cell treated with antibodies directed to rat brain α_{1A}. Shown are distal (A), central (B), and proximal (C) *z*-axis optical sections and a projection of the three (D) as in Fig. 2. Scale bar is 5 μm.

show similar patterns of puncta at the apical tip and along the concave ventral surface of the sperm head. The appearance of some puncta at the same location in adjacent sections presumably indicates that the larger size of α_{1A} puncta allows their detection at both focal planes. The projection of this *z*-series (Fig. 5D) shows that, unlike α_{1C} and α_{1E}, α_{1A} is absent from the acrosomal crescent, but present at the equatorial segment and in the posterior head.

Figure 3E shows that α_{1A} puncta have a distribution in the flagellum which also differs from that of α_{1C} and α_{1E} (Figs. 3A, 3B, 3C, and 3D). Puncta are irregularly arrayed along both the midpiece and the principal piece.

Detection and Characterization of α_1 Subunit Proteins in Sperm Extracts

Figure 6A shows immunoblot analysis of sperm extracts probed with the same antibodies used for immunoimaging (Figs. 1–5). As shown previously (Hell *et al.*, 1993) antibody CNC1 detects ~190- and ~220-kDa α_{1C} bands in affinity-purified preparations of rat brain Ca channels (Fig. 6, lane 1). In sperm extracts, CNC1 recognizes a component migrating at ~200 kDa (lane 2). CNE2 (lane 3) and CNA5 (lane 4) detect single ~245- and ~220-kDa sperm components, consistent with known masses of rat brain α_{1E} and α_{1A} subunits (Catterall *et al.*, 1998). Hence, sperm possess immunoreactive peptides of M_r expected for α_{1C}, α_{1E}, and α_{1A} subunits.

However, lane 2 in Fig. 6 shows that sperm extracts also contain a smaller (~110-kDa) α_{1C}-immunoreactive peptide, not found in rat brain Ca channel preparations. The mobility of this peptide is similar to that of the phosphorylated precursor of mouse sperm fibrous sheath component AKAP82 (Johnson *et al.*, 1997b). Therefore we considered the possibility that localization of α_{1C} puncta in the principal piece could result from cross-reactivity of CNC1 antibody with AKAP82 or its precursor.

In Fig. 6B, immunoblots of purified mouse sperm AKAP82 were probed with CNC1, CNE2, CNA5, and anti-AKAP82 antibodies. A previously described anti-AKAP82 antibody (Johnson *et al.*, 1997b) detected 50, 5, and

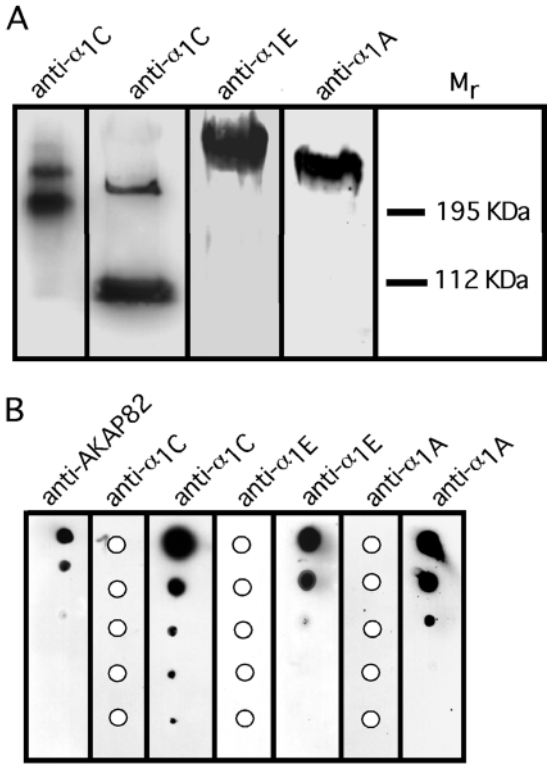

FIG. 6. Immunoblot analysis of sperm Ca channel α_1 subunits and anchoring proteins. (A) Affinity-purified rat brain Ca channels (lane 1) and extracts of whole rat sperm (lanes 2–4) were fractionated by SDS–PAGE, transferred to nitrocellulose, and probed with antibodies directed to α_{1C} (lanes 1 and 2), α_{1E} (lane 3), or α_{1A} (lane 4). (B) Mouse sperm AKAP82 (lanes 1,2,4, and 6), or the α_{1C} peptide antigen for CNC1 (lane 3), the α_{1E} peptide antigen for CNE2 (lane 5), and the α_{1A} peptide antigen for CNA5 (lane 7) were blotted at 50, 5, and 0.5 ng or 50 and 5 pg (rows 1–5, top to bottom) onto nitrocellulose. Anti-AKAP82 antibody probed lane 1, anti-α_1 antibodies CNC1 probed lanes 2 and 3, CNE2 probed lanes 4 and 5, and CNA5 probed lanes 6 and 7.

0.5 ng of applied AKAP82 antigen (lane 1, top three rows). The anti-α_1 antibodies CNC1, CNE2, and CNA5 also detected <1 ng of their antigens (lanes 3, 5, and 7). The sensitivity of CNC1 extended into the low picogram range (lane 3, rows 4 and 5). However, the CNC1, CNE2, and CNA5 antibodies failed to detect AKAP82 at all (lanes 2, 4, and 6). These results indicate that the Ca channel antibodies used in this study do not cross-react significantly with AKAP82 and suggest that the immunoreactive 110-kDa band detected in immunoblots of sperm extracts is not AKAP82 or its precursor.

DISCUSSION

The failure of fertilization in the nominal absence of extracellular Ca^{2+} was recognized nearly a century ago (Lillie, 1913), and the specific defect, a lack of the sperm acrosome reaction, was identified four decades later (Dan, 1954). Later work established that net entry of Ca^{2+} accompanies spontaneous acrosomal exocytosis in vitro (Singh *et al.,* 1978) and that increases in free intracellular [Ca^{2+}] mediate the acrosomal exocytosis evoked by agonists associated with the mammalian egg (Florman *et al.,* 1989, 1992; Thomas and Meizel, 1989). Other studies found that depolarization of sperm in alkaline media elicits an entry of Ca^{2+} (Babcock and Pfeiffer, 1987) and acrosomal exocytosis (Florman *et al.,* 1992; Bramdelli *et al.,* 1996) which are sensitive to dihydropyridines and other inhibitors of L-type voltage-gated Ca channels. The acrosome reaction evoked by the physiological ZP3 agonist displays a similar pharmacological profile. As predicted, sperm membranes contain low-abundance, high-affinity dihydropyridine binding sites (Florman *et al.,* 1992) and, after fusion with lipid bilayers, produce cation currents with some of the properties expected of L-type channels (Tiwari-Woodruff and Cox, 1995). Thus, a relatively complete chain of evidence links activation of sperm L-type Ca channels to the acrosomal exocytosis required for fertilization.

Definitive identification of Ca channels requires knowledge of their molecular and biophysical properties obtained by molecular cloning and biochemical isolation and by characterization with immunological and patch clamp methods. Application of patch clamp and cloning strategies to germ-line cells showed that α_{1A} and α_{1E} mRNA and T-type currents are present in spermatocytes and round spermatids and led to the proposal that mature sperm must possess a similar, highly restricted complement of Ca channels (Hagiwara and Kawa, 1986; Santi *et al.,* 1996; Liévano *et al.,* 1996; Arnoult *et al.,* 1996, 1997). However, the presence of these channels in mature sperm has not been demonstrated previously.

Here we establish that rodent sperm indeed possess α_{1E} subunit proteins and find that the sperm's repertoire of Ca channel proteins additionally includes α_{1C} and α_{1A}. Consistent with these results, Goodwin *et al.* (1997, 1998) recently cloned a unique alternate-splice variant of the α_{1C} transcript previously detected in rat testis (Snutch *et al.,* 1991) and observed immunostaining of rat and human sperm with antibodies directed to skeletal muscle α_1 subunits.

Molecular Properties of Ca Channels of Mature Sperm

The α_{1C} gene contains 44 invariant and at least 6 alternative exons (Soldatov, 1994). The testes α_{1C} variant (Goodwin *et al.* 1997, 1998) most closely resembles the rat brain rB1 clone, and its predicted 2138-amino-acid sequence contains the octadecapeptide used to generate the CNC1 antibody used in the present study. Presumably, conservation of this sequence allows detection of α_{1C} in mouse sperm.

The α_{1C} subunits isolated from brain exist in two sizes (Hell *et al.,* 1993; Catterall *et al.,* 1998). The predominant smaller (190-kDa) form results from truncation of the

COOH-terminal cytosolic tail of the larger (220-kDa) minor form. With rat sperm extracts only a single band of intermediate size (~200 kDa) migrates in this region. Thus it is likely that α_{1C} subunits of brain and testes are processed differently or are differentially degraded during preparation. The significance of the smaller (~110-kDa) α_{1C} component detected in rat sperm extracts is unclear. We have excluded the possibility that its detection results from immunological cross-reactivity with AKAP82, a peptide of similar size and localization in the flagellar principal piece. Proteolytic processing, such as occurs for brain α_{1C} upon activation of the NMDA receptor (Hell *et al.*, 1996), might explain the origin of the 100-kDa component.

At least five splice variants of α_{1E} are known (Marubio *et al.*, 1996). All encode peptides of 220–240 kDa, similar to the mobility of the α_{1E} band detected in rat sperm extracts. No sequence information is yet available for the α_{1E} or α_{1A} transcripts detected in mouse germ line cells (Liévano *et al.*, 1996).

Formation and Maintenance of Regional Localizations of Sperm Ca Channels

The timing of expresssion during spermiogenesis has been proposed to determine the regional distributions of several sperm surface proteins (Cowan and Myles 1993; Cowan *et al.*, 1997). If these considerations also apply to Ca channel proteins, then the local distributions observed in the present study indicate that expression of α_{1E} and α_{1C} occurs both early and late in this process.

Restriction of α_1 subunits to the discrete puncta observed here presumably requires additional mechanisms. Neuronal α_{1A} and α_{1B} subunits contain a "synprint" domain that binds directly to SNARE proteins of the synaptic plasma membrane, thereby ensuring colocalization to synaptic vesicle docking sites and efficient delivery of the Ca^{2+} signal for exocytosis (Sakurai *et al.*, 1996; Kim and Catterall, 1997). The involvement of SNARE proteins in acrosomal exocytosis (Schulz *et al.*, 1997) suggests that α_{1A} localization to the apical tip and equatorial segment of the sperm head may have a similar basis and serve a similar purpose.

The same synprint-containing domain (the cytosolic SII-SIII linker) also specifies association of α_{1C} and α_{1S} with Ca^{2+} release channels of the sarcoplasmic reticulum (see Tanabe *et al.*, 1990). Such association is required for excitation–contraction coupling and for expression of α_{1C} or α_{1S} fusion proteins in punctate foci (Grabner *et al.*, 1998). This region of the sperm α_{1C} and α_{1A} therefore might mediate acrosomal localization by an interaction with other proteins that participate in exocytosis.

In striated muscle L-type Ca channels are functionally coupled to, and presumably colocalized with, signaling complexes that contains protein kinases and anchoring proteins (Gao *et al.*, 1997; Gray *et al.*, 1997; Johnson *et al.*, 1997a). The patterns of α_{1C} puncta in the sperm flagellum resemble those reported for the anchoring protein AKAP82 (Johnson *et al.*, 1997b), suggesting that formation of analogous signaling complexes may localize α_{1C} and α_{1E} Ca channel subunits to the puncta observed along the flagellar principal piece.

Possible Functional Roles of Sperm Ca Channels

We find that rodent sperm possess probable homologs to the α_{1A}, α_{1C}, and α_{1E} subunits that determine the properties of Ca channels in other cells. Both α_{1C} and α_{1E} subunits are found on the dorsal aspect of the acrosomal crescent of mouse sperm, presumably in the surface membranes that overlie the acrosome, where their activation may initiate exocytosis. The less-restricted localization of α_{1E} in the anterior head suggests that it may have other or additional roles, for instance in the glycolipid redistribution that occurs during sperm capacitation (Gadella *et al.*, 1995). At present, lack of a well-defined pharmacology and an inability to apply patch clamp methods preclude definitive determination of the functional status, properties, and roles of sperm α_{1C} and α_{1E}.

Two groups (Meizel *et al.*, 1997; Miyazaki and Shirakawa, 1997) report that a wave of elevated $[Ca^{2+}]_i$ progresses from the equatorial segment during acrosomal exocytosis. Puncta of α_{1A} located at this site might participate in this initiating ionic event. The α_{1A} puncta found in the postacrosomal head presumably would be retained after the acrosome reaction and might then function in events more closely associated with gamete fusion. The unique presence of α_{1A} over the sperm midpiece could provide a pathway for selective access of Ca^{2+} to the sperm mitochondria, perhaps to regulate metabolic activity.

Much evidence indicates that sperm swimming behavior is altered by an entry of Ca^{2+} that occurs prior to contact with the egg. For sea urchins, chemotactic oligopeptides from the egg engage sperm signaling pathways thought to indirectly activate voltage-gated Ca channels (Cook and Babcock, 1993; Cook *et al.*, 1994). The Ca^{2+}-dependent responses of sperm to electrical field stimulation (Shigyoji and Takahashi, 1995) support this interpretation. For mammalian sperm, Ca^{2+} also controls flagellar waveform, but no chemotactic agonists have been identified. The presence of α_{1C} and α_{1E} on the sperm flagellum suggests that voltage-gated Ca channels may provide paths for Ca^{2+} entry to produce the flagellar beat asymmetry observed during sperm hyperactivation and expected during chemotactic responses. However, the cyclic nucleotide-gated channels also present on the flagellum could serve as alternate routes (Wiesner *et al.*, 1998).

In summary, we have provided immunocytochemical evidence that rodent sperm contain the pore-containing subunits of L-, P/Q-, and R- or T-type Ca channels. We also have shown that these Ca channel proteins have distinct, discrete localization patterns in epididymal sperm. It is quite remarkable that the extreme functional polarization of sperm is reflected in this localization of Ca channel subtypes. The basis for these distributions, whether they can provide routes for selective control of Ca^{2+} entry and

modulation of exocytotic, metabolic, and kinetic activity, and how they are affected by the membrane remodeling and other alterations that occur as capacitating sperm prepare for fertilization, are all intriguing topics for future study.

ACKNOWLEDGMENTS

This research was supported by HD12629 and The W. M. Keck Foundation. We are grateful to Drs. B. Hille and W. A. Catterall for providing laboratory space and continued encouragement for this work. We thank Dr. S. B. Moss for sperm AKAP82 and anti-AKAP82 antibody. We also thank Drs. J. Isaacson, J. Koehler, and T. Scheuer for helpful comments.

REFERENCES

Anhlijanian, M. K., Westenbroek, R. E., and Catterall, W. A. (1990). Subunit structure and localization of dihydropyridine-sensitive calcium channels in mammalian brain, spinal cord, and retina. *Neuron* **4,** 819–832.

Arnoult, C., Cardullo, R. A., Lemos, J. R., and Florman, H. M. (1996). Egg activation of sperm T-type Ca^{2+} channels regulates acrosome reactions during mammalian fertilization. *Proc. Natl. Acad. Sci. USA* **93,** 13004–13009.

Arnoult, C., Lemos, J. R., and Florman, H. M. (1997). Voltage-dependent modulation of T-type calcium channels by protein tyrosine phosphorylation. *EMBO J.* **16,** 1593–1599.

Babcock, D. F., and Pfeiffer, D. R. (1987). Independent elevation of cytosolic [Ca^{2+}] and pH_i of mammalian sperm by voltage-dependent and pH sensitive mechanisms. *J. Biol. Chem.* **262,** 15041–15047.

Babcock, D. F., Bosma, M., Battaglia, D. E., and Darszon, A. (1992). Early persistent activation of sperm K^+ channels by the egg peptide speract. *Proc. Natl. Acad. Sci. USA* **89,** 6001–6005.

Bartles, J. R. (1996). The spermatid plasma membrane comes of age. *Trends Cell. Biol.* **5,** 400–404.

Berruti, G., and Borgonovo, B. (1996). sp42, the boar sperm tyrosine kinase, is a male germ cell-specific product with a highly conserved tissue expression extending to other mammalian species. *J. Cell Sci.* **109,** 851–858.

Bourinet, E., Zamponi, G. W., Stea, A., Soong, T. W., Lewis, B. A., Jones, L. P., Yue, D. T., and Snutch, T. P. (1996). The alpha-1E calcium channel exhibits permeation properties similar to low-voltage-activated calcium channels. *J. Neurosci.* **16,** 4983–4993.

Bramdelli, A., Miranda, P. V., and Tezon, J. G. (1996). Voltage-dependent calcium channels and G_i regulatory protein mediate the human sperm acrosomal exocytosis induced by *N*-acetylglucosaminyl/mannosyl neoglycoproteins. *J. Androl.* **17,** 522–529.

Carrera, A., Gerton, G. L., and Moss, S. B. (1994). The major fibrous sheath polypeptide of mouse sperm: Structural and functional similarities to the A-kinase anchoring proteins. *Dev. Biol.* **165,** 272–284.

Catterall, W. A., Westenbroek, R. E., Herlitze, S., and Yokoyama, C. T. (1998). Localisation and function of brain calcium channels. *In* "Low-Voltage-Activated T-Type Calcium Channels" (R.W. Tsien, J.-P. Clozel, and J. Nargeot, Eds.), pp. 207–217. Adis International, Chester, UK.

Cook, S. P., and Babcock, D. F. (1993). Activation of Ca^{2+} permeability by cAMP is coordinated through the pH_i increase induced by speract. *J. Biol. Chem.* **268,** 22408–22413.

Cook, S. P., Brokaw, C. J., Muller, C. H., and Babcock, D. F. (1994). Sperm chemotaxis: Egg peptides control calcium to regulate flagellar responses. *Dev. Biol.* **165,** 10–19.

Cowan, A. E., and Myles, D. G. (1993). Biogenesis of surface domains during spermiogenesis in the guinea pig. *Dev. Biol.* **155,** 124–133.

Cowan, A. E., Nakhimovsky, L., Myles, D. G., and Koppel, D. E. (1997). Barriers to diffusion of plasma membrane proteins form early during guinea pig spermiogenesis. *Biophys. J.* **73,** 507–516.

Cribbs, L. L., Lee, J.-H., Yang, J., Satin, J., Zhang, Y., Daud, A., Barclay, J., Williamson, M. P., Fox, M., Rees, M., and Perez-Reyes, E. (1998). Cloning and characterization of α1H from human heart, a member of the Ca^{2+} gene family. *Circ. Res.* **83,** 103–109.

da Cruz e Silva, E. F., Fox, C. A., Quimet, C. C., Gustafson, E., Watson, S. J., and Greengard, P. (1995). Differential expression of protein phosphatase 1 isoforms in mammalian brain. *J. Neurosci.* **15,** 3375–3389.

Dan, J. C. (1954). Studies on the acrosome. III. Effect of calcium deficiency. *Biol. Bull.* **107,** 335–349.

DeJongh, K. S., Murphy, M. J., Colvin, A. A., Hell, J. W., Takahashi, M., and Catterall, W. A. (1996). Specific phosphorylation of a site in the full-length form of the α_1 subunit of the cardiac L-type calcium channel by adenosine 3′,5′-cyclic monophosphate-dependent protein kinase. *Biochemistry* **35,** 10392–10402.

De Waard, M., Gurnett, C. A., and Campbell, K. P. (1996). Structural and functional diversity of voltage-activated calcium channels. *In* "Ion Channels", (T. Narahashi, Ed.), Vol. 4, pp. 41–87, Plenum, New York.

Eddy, E. M., and O' Brien, D. A. (1994). The spermatozoon. *In* "The Physiology of Reproduction" (E. Knobil and J. D. Neill, Eds.), pp.29–79. Raven Press, New York.

Fawcett, D. W. (1975). The mammalian spermatozoon. *Dev. Biol.* **44,** 394–436.

Florman, H. M., Tombes, R. M., First, N. L., and Babcock, D. F. (1989). An adhesion-associated agonist from the zona pellucida activates G protein-promoted elevations of internal Ca^{2+} and pH that mediate mammalian sperm acrosomal exocytosis. *Dev. Biol.* **135,** 133–146.

Florman, H. M., Corron, M., Kim, T., and Babcock, D. F. (1992). Activation of voltage-dependent calcium channels in mammalian sperm is required for zona pellucida-induced acrosomal exocytosis. *Dev. Biol.* **152,** 304–314.

Gadella, B. M., Lopez-Cardozo, M., van Golde, L. M. G., Colenbrander, B., and Gadella, T. M. J., Jr. (1995). Glycolipid migration from the apical to the equatorial subdomains of the sperm head plasma membrane precedes the acrosome reaction. Evidence for a primary capacitation event in boar spermatozoa. *J. Cell Sci.* **108,** 935–945.

Gao, T., Yatani, A., Dell'Acqua, M. L., Sako, H., Green, S. A., Dascal, N., Scott, J. D., and Hosey, M. M. (1997). cAMP-dependent regulation of cardiac L-type Ca^{2+} channels requires membrane targeting of PKA and phosphorylation of channel subunits. *Neuron* **19,** 185–196.

Goodwin, L. O., Leeds, N. B., Hurley, I., Mandel, F. S., Pergolizzi, R. G., and Benoff, S. (1997). Isolation and characterization of the primary structure of testis-specific L-type calcium channel: Implications for contraception. *Mol. Hum. Reprod.* **3,** 255–268.

Goodwin, L. O., Leeds, N. B., Hurley, I., Cooper, G. W., Pergolizzi, R. G., and Benoff, S. (1998). Alternative splicing of exons in the α1 subunit of the rat testis L-type voltage-dependent calcium channel generates germ line-specific dihydropyridine binding sites. *Mol. Hum. Reprod.* **4,** 215–226.

Grabner, M., Dirksen, R. T., and Beam, K. G. (1998). Tagging with green fluorescent protein reveals a distinct subcellular distribution of L-type and non-L-type Ca^{2+} channels expressed in dysgenic myotubes. *Proc. Natl. Acad. Sci. USA* **95,** 1903–1908.

Gray, P. C., Tibbs, V. C., Catterall, W. A., and Murphy, B. J. (1997). Identification of a 15-kDa cAMP-dependent protein kinase-anchoring protein associated with skeletal muscle L-type calcium channels. *J. Biol. Chem.* **272,** 6297–6302.

Hagiwara, S., and Kawa, K. (1984). Calcium and potassium currents in spermatogenic cells dissociated from rat seminiferous tubules. *J. Physiol.* **356,** 135–149.

Hell, J. W., Yokoyama, C. T., Wong, S. T., Warner, C., Snutch, T. P., and Catterall, W. A. (1993). Differential phosphorylation of two size forms of the neuronal class C L-type calcium channel alpha 1 subunit. *J. Biol. Chem.* **268,** 19451–19457.

Hell, J. W., Westenbroek, R. E., Breeze, L. J., Wang, K. K., Chavkin, C., and Catterall, W. A. (1996). *N*-Methyl-D-aspartate receptor-induced proteolytic conversion of post synaptic class C, L-type calcium channels in hippocampal neurons. *Proc. Natl. Acad. Sci. USA* **93,** 3362–3367.

Johnson, B. D., Brousal, J. P., Peterson, B. Z., Gallombardo, P. A., Hockerman, G. H., Lai, L., Scheuer, T., and Catterall, W. A. (1997a). Modulation of the cloned skeletal muscle L-type Ca^{2+} channel by anchored cAMP-dependent protein kinase. *J. Neurosci.* **15,** 243–1255.

Johnson, L. R., Foster, J. A., Haig-Ladewig, L., VanScoy, H., Rubin, C. S., Moss, S. B., and Gerton, G. L. (1997b). Assembly of AKAP82, a protein kinase anchor protein, into the fibrous sheath of mouse sperm. *Dev. Biol.* **192,** 340–350.

Kim D. K., and Catterall, W. A. (1997). Ca^{2+}-dependent and -independent interactions of the isoforms of the alpha1A subunit of brain Ca^{2+} channels with presynaptic SNARE proteins. *Proc. Natl. Acad. Sci. USA* **94,** 14782–14786.

Lieberman, S. J., Wasco, W., MacLeod, J., Satir, P., and Orr, G. A. (1988). Immunogold localization of the regulatory subunit of a type II cAMP-dependent protein kinase tightly associated with mammalian sperm flagella. *J. Cell Biol.* **107,** 1809–1816.

Liévano, A., Santi, C. M., Serrano, C. J., Treviño, C. L., Bellvé, A. R., Hernández-Cruz, A., and Darszon, A. (1996). T-type Ca^{2+} channels and α_{1E} expression in spermatogenic cells, and their possible relevance to the sperm acrosome reaction. *FEBS Lett.* **388,** 150–154.

Lillie, F. R. (1913). Studies of fertilization. V. The behavior of spermatozoa of *Nereis* and *Arbacia* with special reference to egg extractives. *J. Exp. Zool.* **16,** 515–574.

Marubio L. M., Röenfeld, M., Dasgupta, S., Miller, R. J., and Philipson, L. H. (1996). Isoform expression of the voltage-dependent calcium channel α_{1E}. *Receptors Channels* **4,** 243–251.

Mei, X., Singh, I. S., Ehrlichman, J., and Orr, G. A. (1997). Cloning and characterization of a testis-specific, developmentally regulated A-kinase anchoring protein (TAKAP-80) present on the fibrous sheath of rat sperm. *Eur. J. Biochem.* **246,** 425–432.

Meir, A., and Dolphin, A. C. (1998). Known calcium channel alpha1 subunits can form low threshold small conductance channels with similarities to native T-type channels. *Neuron* **20,** 341–51.

Meizel, S., Turner, K. O., and Nucitelli, R. (1997). Progesterone triggers a wave of increased free calcium during the human sperm acrosome reaction. *Dev. Biol.* **182,** 67–75.

Miyazaki, S., and Shirakawa, H. (1997). Spatiotemporal analysis of calcium dynamics in hamster spermatozoa during acrosome reaction observed with confocal microscopy. *XXXIII Int. Congr. Physiol. Sci.,* P012.11a.

Naro, F., Zhang, R., and Conti, M. (1996). Developmental regulation of unique adenosine 3′,5′-monophosphate-specific phosphodiesterase variants during rat spermatogenesis. *Endocrinology* **137,** 2464–2472.

Perez-Reyes, E., Cribbs, L. L., Daud, A., Lacerda, A. E., Barclay, J., Williamson, M. P., Fox, M., Rees, M., and Lee, J. H. (1998). Molecular characterization of a neuronal low-voltage-activated T-type calcium channel. *Nature* **391,** 896–900.

Randall, A. D., and Tsien, R. W. (1997). Contrasting biophysical and pharmacological properties of T-type and R-type calcium channels. *Neuropharmacology* **36,** 879–893.

Sakurai T., Westenbroek, R. E., Rettig, J., Hell, J., and Catterall, W. A. (1996). Biochemical properties and subcellular distribution of the BI and rbA isoforms of alpha 1A subunits of brain calcium channels. *J. Cell Biol.* **134,** 511–528.

Sallese, M. S., Mariggio, S., Collodel, G., Moretti, E., Piomboni, P., Baccetti, B., and De Blasi, A. (1997). G protein-coupled receptor kinase GRK4. Molecular analysis of the four isoforms and ultrastructural localization in spermatozoa and germinal cells. *J. Biol. Chem.* **272,** 10188–10195.

Santi, C. M., Darszon, A., and Hernández-Cruz, A. (1996). A dihydropryridine-sensitive T-type Ca^{2+} current is the main Ca^{2+} current carrier in mouse primary spermatocytes. *Am J. Physiol.* **271,** C1583–C1593.

Schulz, J. R., Wessel, G. M., and Vacquier, V. D. (1997). The exocytosis regulatory proteins syntaxin and VAMP are shed from sea urchin sperm during the acrosome reaction. *Dev. Biol.* **191,** 80–87.

Shigyoji, C., and Takahashi, K. (1995). Flagellar quiescence response in sea urchin sperm induced by electric stimulation. *Cell Motil. Cytoskel.* **31,** 59–65.

Singh, J. P., Babcock, D. F., and Lardy, H. A. (1978). Increased Ca^{++} influx is a component of sperm capacitation. *Biochem. J.* **172,** 549–556.

Snell, W. J., and White, J. M. (1996). The molecules of mammalian fertilization. *Cell* **85,** 629–637.

Snutch, T. P., Tomlinson, W. J., Leonard, J. P., and Gilbert, M. M. (1991). Distinct calcium channels are generated by alternative splicing and are differentially expressed in the mammalian CNS. *Neuron* **7,** 45–57.

Soldatov, N. M. (1994). Genomic structure of human L-type Ca^{2+} channel. *Genomics* **22,** 77–87.

Tanabe, T., Beam, K. G., Adams, B. A., Niidome, T., and Numa, S. (1990). Regions of the skeletal muscle dihydropyridine receptor critical for excitation–contraction coupling. *Nature* **346,** 567–569.

Thomas, P., and Meizel, S. (1989). Phosphatidylinositol 4,5-bisphosphate hydrolysis in human sperm stimulated with follicular fluid or progesterone is dependent upon Ca^{2+} influx. *Biochem. J.* **264,** 539–546.

Tiwari-Woodruff, S. K., and Cox, T. C. (1995). Boar sperm plasma membrane Ca^{2+}-selective channels in planar lipid bilayers. *Am J. Physiol.* **268,** C1284–C1294.

Toshimori, K., Higashi, R., and Oura, C. (1985). Distribution of intramembranous particles and filipin-sterol complexes in

mouse sperm membranes: Polyene antibiotic filipin treatment. *Am. J. Anat.* **174,** 455–470.

Vijayaraghavan, S., Olson, G. E., NagDas, S., Winfrey, V. P., and Carr, D. W. (1997). Subcellular localization of the regulatory subunits of cAMP-dependent protein kinase in bovine spermatozoa. *Biol. Reprod.* **57,** 1517–1523.

Walensky, L. D., Roskams, A. J., Lefkowitz, R. J., Snyder, S. H., and Ronnett, G. V. (1996). Odorant receptors and desensitization proteins colocalize in mammalian sperm. *Mol. Med.* **1,** 130–141.

Ward, C. R., and Kopf, G. S. (1993). Molecular events mediating sperm activation. *Dev. Biol.* **158,** 9–34.

Westenbroek, R. E., Hell, J. W., Warner, C., Dubel, S. J., Snutch, T. P., and Catterall, W. A. (1992). Biochemical properties and subcellular distribution of an N-type calcium channel alpha 1 subunit. *Neuron* **6,** 1099–1115.

Wiesner, B., Weiner, J., Middendorff, R., Hagen, V., Kaupp, U. B., and Weyand, I. (1998). Cyclic nucleotide-gated channels on the flagellum control Ca^{2+} entry into sperm. *J. Cell Biol.* **142,** 473–484.

Yokoyama, C., Westenbroek, R. E., Hell, J. W., Soong, T. K., Snutch, T. P., and Catterall, W. A. (1995). Biochemical properties and subcellular distribution of the neuronal class E calcium channel α_1 subunit. *J. Neurosci.* **15,** 6419–6432.

Zini, N., Matteucci, A., Sabatelli, P., Valmori, A., Carmelli, E., and Maraldi, N. M. (1997). Protein kinase C isoforms undergo quantitative variations during rat spermatogenesis and are selectively retained at specific spermatozoon sites. *Eur. J. Cell Biol.* **72,** 142–150.

Received for publication September 4, 1998
Revised December 7, 1998
Accepted December 10, 1998